DETC2002/MECH-34261

SPASUR: INTERACTIVE VISUALIZATION OF THE COUPLER SURFACES OF THE SPATIAL 4C MECHANISM

Pierre M. Larochelle∗
Robotics and Spatial Systems Laboratory
Mechanical and Aerospace Engineering Department
Florida Institute of Technology
Melbourne, Florida 32901
Email: pierrel@fit.edu

Agnes Agius
Robotics and Spatial Systems Laboratory
Mechanical and Aerospace Engineering Department
Florida Institute of Technology
Melbourne, Florida 32901
Email: aagius@fit.edu

ABSTRACT

This paper presents a software tool entitled *SPASUR* (SPAtial SURface) for the interactive visualization of the coupler surfaces of the spatial 4C mechanism. The 4C mechanism is a two degree of freedom spatial four-bar linkage. The path traced by a point attached to the coupler or floating link defines a surface in space. An interactive graphical user interface has been created and integrated with kinematic analysis routines to generate and display these coupler surfaces. The result is a user-friendly and efficient means of generating and visualizing the coupler surfaces of the spatial 4C four-bar mechanism.

1 INTRODUCTION

In this paper we present a parameterized representation of the coupler surface of a spatial 4C four-bar mechanism, see Fig. 1. The methodology utilizes an analytic representation of the linkage's coupler point position that is parameterized by the mechanism's joint variables (i.e. rotation angles and translational distances). The kinematic analysis of the kinematic closed chain is utilized to eliminate all but two joint variables. The result is a representation of the coupler surface associated with a coupler point on a spatial four-bar mechanism that is parameterized by its two driving joint variables.

Recently, there have been some significant efforts made to address the challenge of designing useful spatial mechanisms.

In (Larochelle, 1998) a Burmester Theory based computer-aided design program for spatial 4C mechanisms was reported. Efforts were made to address circuit and branch defects in (Larochelle, 2000). Approximate motion synthesis was addressed in (Larochelle, 1994) and (Dees, 2001). The exploration of utilizing virtual reality techniques to address the inherent visualization and interaction challenges was reported in (Kihonge et al, 2002). Moreover, the work reported here was motivated to a large extent by the study of the coupler curves of the RCCC mechanism reported by (Marble and Pennock, 1999). They used a dual-number approach to generate parametric equations of the coupler curves of RCCC spatial four-bar mechanisms. Furthermore, Marble and Pennock proved that the polynomial describing the coupler curve is 16th degree. Here, we build upon their work and examine the coupler surfaces of the 4C mechanism.

The immediate goal here was to create an interactive visualization tool to represent the coupler surfaces of the spatial 4C mechanism. This is one step toward the long term goal of creating an interactive computer-aided design software tool to synthesize spatial 4C mechanisms for prescribed coupler surfaces. Such mechanisms would be applicable wherever complex surface motions are required and/or manufactured; such as in freeform modeling and manufacturing, mold and pattern making, surface finishing, etc. Consider this conceptual example of freefrom manufacturing, a NURBS based software (e.g. Rhinoceros™) could be used to design and prescribe a desired complex freeform surface. A spatial 4C mechanism could then be synthesized such that its coupler surface includes the prescribed surface. Finally,

---

∗Address all correspondence to this author.
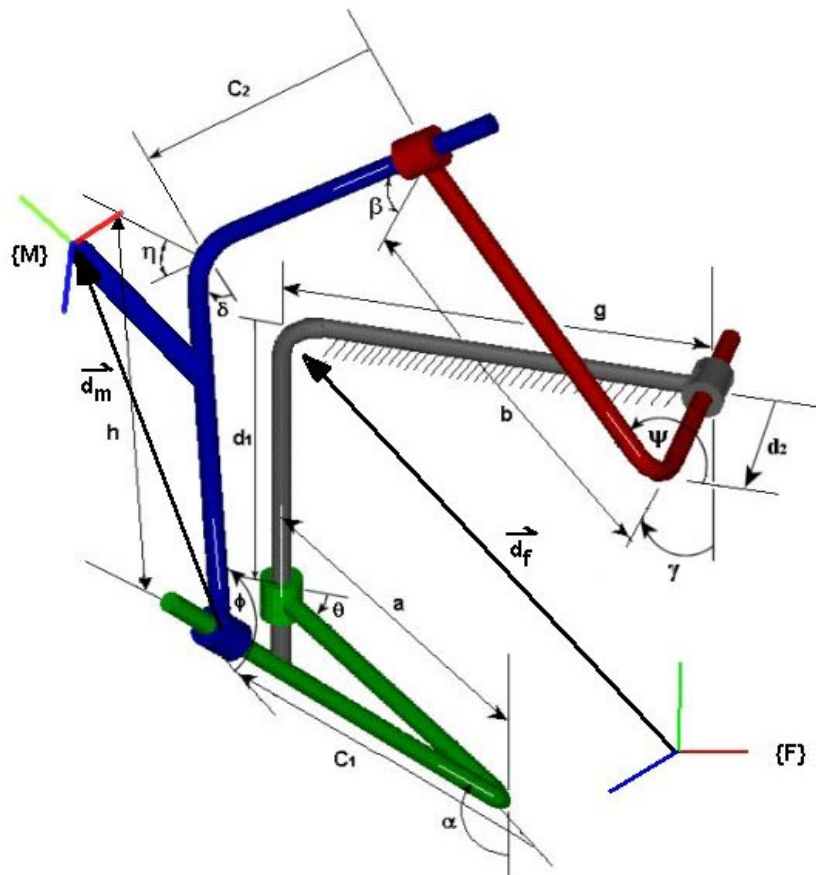
Figure 1.   SPATIAL 4C MECHANISM

the freeform surface could be manufactured via material removal from raw stock by attaching a cutting tool to the coupler of the mechanism such that the tip of a cutting tool is coincident with the coupler point. Let us consider another conceptual example, the design and manufacture of a complex automobile quarter-panel. These surfaces are often generated with freeform surface design software programs. A spatial 4C mechanism could be designed such that its coupler point traces the prescribed surface. Such a mechanism could be applicable to: (1) making the patterns/dies used to manufacture the quarter-panels, (2) surface finishing of the quarter-panels (grinding, sanding, and/or painting, etc.), and, (3) inspecting the finished quarter-panels (e.g. ccd cameras, touch probes, etc.).

The paper proceeds as follows. First, the necessary kinematic analyses of the spatial 4C mechanism are performed. Next, utilizing the results of the analyses we generate the parametric representation of the coupler surface of the spatial 4C mechanism. Finally, the interactive visualization program *SPASUR* is presented as well as images of example coupler surfaces.

2 THE SPATIAL 4C MECHANISM

A spatial 4C mechanism has four cylindrical joints, each joint permitting relative rotation and translation along a line, see Fig. 1. The link parameters that define the mechanism are listed in Tbl. 1 and the joint variables are defined in Tbl. 2.

The spatial 4C mechanism may be viewed as a combination of two CC dyads. The driving CC dyad has four independent joint variables, referred to as θ, d_1, ϕ and c_1. The driven dyad also has four independent joint variables, ψ, d_2, δ and c_2. When adjoined by the coupler link, the two dyads form a closed chain spatial 4C mechanism with two degrees of freedom. We chose θ and d_1 to be the independent joint variables. Note that ϕ and c_1 as well as the driven dyad's joint variables are now explicit functions of θ and d_1 and these functions are found below.

2.1 Spatial 4C Mechanism Analysis

We now present the equations that define the relative movement for the links of a spatial 4C mechanism given its physical dimensions and the input variables, θ and d_1. The closed chain vector loop equations were solved to yield the following equa-

2

tions, (Larochelle, 1998).

The coupler angle ϕ as a function of the input angle θ is

$$\phi(\theta) = \arctan\left(\frac{B}{A}\right) \pm \arccos\left(\frac{C}{\sqrt{A^2 + B^2}}\right) \qquad (1)$$

where

$$A = \sin(\eta)\sin(\gamma)\cos(\alpha)\cos(\theta) -$$
$$\sin(\alpha)\sin(\eta)\cos(\gamma)$$
$$B = -\sin(\eta)\sin(\gamma)\sin(\theta)$$
$$C = \cos(\beta) - \cos(\eta)\sin(\alpha)\sin(\gamma)\cos(\theta) -$$
$$\cos(\alpha)\cos(\eta)\cos(\gamma).$$

Note that ϕ has two solutions corresponding to the two assemblies or circuits of the mechanism.

The output angle ψ as a function of the input angle θ and the coupler angle ϕ is

$$\psi(\theta, \phi) = \arctan\left(\frac{B}{A}\right) \qquad (2)$$

where

$$A = \frac{1}{-\sin(\beta)}\Big\{\cos(\eta)(\cos(\alpha)\sin(\gamma) -$$
$$\cos(\gamma)\cos(\theta)\sin(\alpha)) -$$
$$\sin(\eta)\cos(\phi)(\cos(\alpha)\cos(\gamma)\cos(\theta) +$$
$$\sin(\alpha)\sin(\gamma)) +$$
$$\sin(\eta)\cos(\gamma)\sin(\phi)\sin(\theta)\Big\}$$
$$B = \frac{1}{\sin(\beta)}\Big\{\cos(\eta)\sin(\alpha)\sin(\theta) +$$
$$\sin(\eta)\cos(\theta)\sin(\phi) +$$
$$\sin(\eta)\cos(\alpha)\cos(\phi)\sin(\theta)\Big\}.$$

The output coupler angle δ, i.e. the angle between the coupler and driven crank is

$$\delta(\theta, \psi) = \arctan\left(\frac{B}{A}\right) \qquad (3)$$

where

$$A = \frac{1}{\sin(\eta)}\Big\{\cos(\alpha)\big(\cos(\gamma)\sin(\beta) +$$

Table 1. LINK PARAMETERS OF THE SPATIAL 4C MECHANISM

Link	Dual Angle	Twist	Length
Driving	$\hat{\alpha}$	α	a
Coupler	$\hat{\eta}$	η	h
Driven	$\hat{\beta}$	β	b
Fixed	$\hat{\gamma}$	γ	g

Table 2. JOINT VARIABLES OF THE SPATIAL 4C MECHANISM

Joint	Dual Angle	Rotation	Translation
Driving fixed	$\hat{\theta}$	θ	d_1
Driving moving	$\hat{\phi}$	ϕ	c_1
Driven moving	$\hat{\delta}$	δ	c_2
Driven fixed	$\hat{\psi}$	ψ	d_2

$$\cos(\beta)\sin(\gamma)\cos(\psi)) -$$
$$\sin(\alpha)\cos(\theta)\big(\cos(\beta)\cos(\gamma)\cos(\psi) -$$
$$\sin(\beta)\sin(\gamma)\big) -$$
$$\sin(\alpha)\cos(\beta)\sin(\theta)\sin(\psi)\Big\}$$
$$B = \frac{1}{-\sin(\eta)}\Big\{\cos(\alpha)\sin(\gamma)\sin(\psi) +$$
$$\sin(\alpha)\sin(\theta)\cos(\psi) -$$
$$\sin(\alpha)\cos(\gamma)\cos(\theta)\sin(\psi)\Big\}.$$

Finally, the driving coupler translation c_1, the translation along the driving moving axis, is given by

$$c_1(\theta, \psi, \delta, d_1) = \frac{A}{B} \qquad (4)$$

where

$$A = d_1\sin(\gamma)\sin(\psi) + a\cos(\theta)\cos(\psi)$$
$$+ a\cos(\gamma)\sin(\theta)\sin(\psi) + h\cos(\delta)$$
$$- b - g\cos(\psi)$$
$$B = \sin(\eta)\sin(\delta).$$

2.2 The Parameterized Coupler Surface

We now utilize the solution of the kinematic analysis to derive a parameterized representation of the coupler surface asso-

3   Copyright © 2002 by ASME

ciated with a spatial 4C mechanism. First, we generate a representation of a prescribed coupler point $\vec{p}$ that is parameterized by the driving joint variables θ and d_1. This is done by performing a forward kinematic analysis of the driving dyad,

$$\vec{p}(\theta, d_1) = F \, Z(\theta, d_1) \, X(\alpha, a) \, Z(\phi, c_1) \, \vec{p}_M \qquad (5)$$

where Fig. 2 illustrates the sequence of transformations, $\vec{p}_M$ is the coupler point expressed with respect to the moving frame attached to the coupler and F is the homogeneous transform from the fixed reference frame to the frame attached to the fixed link of the driving dyad. Eq. 5 yields the coupler surface of the spatial 4C mechanisms parameterized by the two driving joint variables θ and d_1 since $\phi(\theta)$ and $c_1(\theta, d_1)$ are given by Eqs. 1 and 4 respectively.
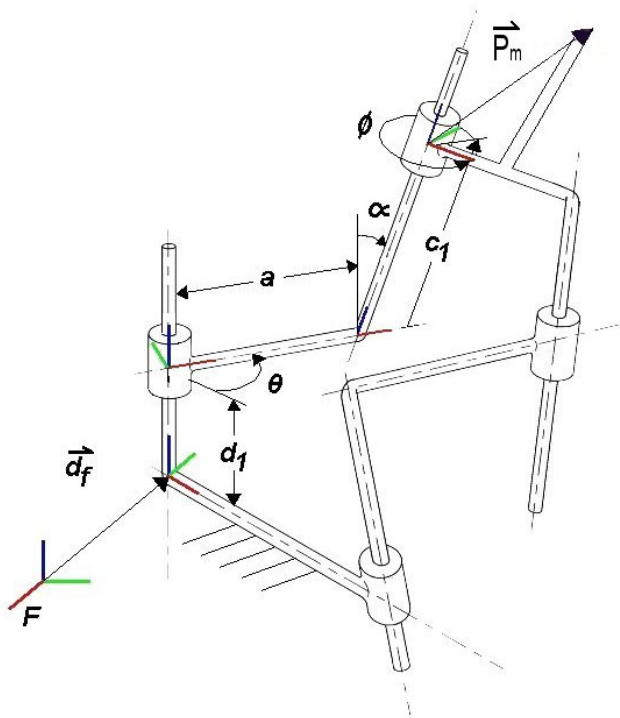
Figure 2. FORWARD KINEMATIC ANALYSIS

2.3 Mechanism Classification

In order to facilitate the visual representation of the coupler surface it is necessary to know the mechanism's classification or type. In the case of spatial 4C mechanisms the angular relationships define the gross motion characteristics and we therefore

Table 3. BASIC SPHERICAL 4R LINKAGE TYPES

	Linkage type	T_1	T_2	T_3	T_4
1.	Crank-rocker	+	+	+	+
2.	Rocker-crank	+	-	-	+
3.	Double-crank	-	-	+	+
4.	Grashof double-rocker	-	+	-	+
5.	$00+$ double-rocker	-	-	-	+
6.	$0\pi+$ double-rocker	+	+	-	+
7.	$\pi 0+$ double-rocker	+	-	+	+
8.	$\pi\pi+$ double-rocker	-	+	+	+
9.	Crank-rocker	-	-	-	-
10.	Rocker-crank	-	+	+	-
11.	Double-crank	+	+	-	-
12.	Grashof double-rocker	+	-	+	-
13.	$00-$ double-rocker	+	+	+	-
14.	$0\pi-$ double-rocker	-	-	+	-
15.	$\pi 0-$ double-rocker	-	+	-	-
16.	$\pi\pi-$ double-rocker	+	-	-	-

employ the spherical image classification scheme of (Murray and Larochelle, 1998). (Duffy, 1980) shows that there is a spherical image associated with each spatial four-bar mechanism. The spherical image is a spherical 4R mechanism having link lengths equal to the angular twists of the 4C mechanism (α, γ, η, β). We utilize the following parameters, introduced by (Murray and Larochelle, 1998), to classify the spherical image of a spatial 4C mechanism

$$\begin{aligned}
T_1 &= \gamma - \alpha + \eta - \beta \\
T_2 &= \gamma - \alpha - \eta + \beta \\
T_3 &= \eta + \beta - \gamma - \alpha \\
T_4 &= 2\pi - \eta - \beta - \gamma - \alpha.
\end{aligned}$$

The four parameters $T_i, i = 1, 2, 3, 4$ classify the movement of the driving and driven links of the spherical 4R linkage into sixteen basic types, see Tbl. 3. Moreover, in terms of these T parameters, the Grashof condition for spherical 4R mechanisms may be stated as $T_1 T_2 T_3 T_4 > 0$. If the Grashof condition is satisfied then one or more links can fully rotate and the mechanism has two distinct assemblies. Most importantly, for each different assembly of a 4C mechanism a distinct and separate coupler surface

exists.

3 *SPASUR*

In this section we present *SPASUR* and visualizations of two example coupler surfaces. First, the analysis methodologies presented above were programmed using MatLab-6 and a simple and efficient user interface was designed, see Figs. 5 and 8. The user interface allows for both the direct entry of numerical data and/or the use of slider bars to permit parametric design studies.

The coupler surfaces are generated by discretizing the range of input translational motion d_1 over a prescribed finite range; in the examples presented here $0 \leq d_1 \leq 100$. For each value of d_1 we vary θ through its allowable range of motion; the mechanism classification scheme presented above is utilized to determine the mechanism's type and valid θ range(s). For each driving joint variable pair (θ, d_1) we generate a distinct coupler surface point $\vec{p}$ by using Eq. 5. Finally, MatLab-6 provides the user with efficient means for interactive visualization of the surfaces including rotating view functions, scaling, and surface rendering, and lighting.

3.1 Spatial 4C Crank-Rocker Mechanism

The coupler surfaces associated with a crank-rocker spatial 4C mechanism are shown in Figs. 3 and 4. Since this is a Grashof mechanism there are two distinct coupler surfaces associated with it as shown in Fig. 3. In Fig. 4 one of the coupler surfaces is shown as well as the joint axes of the spatial 4C mechanism; *black* = driving fixed axis, *green* = driving moving axis, *red* = driven moving axis, and *blue* = driven fixed axis. The data for this mechanism is found in Fig. 5.

3.2 Spatial 4C Double-Rocker Mechanism

The coupler surface associated with a $\pi\pi+$ double-rocker spatial 4C mechanism is shown in Fig. 6. This is a non-Grashof mechanism and there is only one associated coupler surface. Notice that this mechanism reaches translational singular configurations at the limits of its θ motion. In these translational singular configurations $\delta = 0$ *or* π which results in $c_1 \to \infty$; see Eq. 4. The resulting effect on the coupler surface is the *planar* appearing region of the coupler surface. This region is not real and only appears due to the points on the coupler surface approaching ∞. In Fig. 7 the coupler surface is shown again but here the driving angle θ has been bounded to remain 15(deg) away from the limits of its range of motion. Notice that by doing so the mechanism avoids the translational singular configurations that occur at the θ limits; see (Larochelle, 2000) for further discussion of the translational singular configurations of the 4C mechanism. The data for this mechanism is found in Fig. 8.

4 CONCLUSIONS

This paper has presented a software tool entitled *SPASUR* (SPAtial SURface) for the interactive visualization of the coupler surfaces of the spatial 4C mechanism. An interactive graphical user interface has been created and integrated with kinematic analysis routines to generate and display these coupler surfaces. The result is a user-friendly and efficient means of generating and visualizing the coupler surfaces of the spatial 4C four-bar mechanism. This is one step toward the long term goal of creating an interactive computer-aided design software tool to synthesize spatial 4C mechanisms for prescribed coupler surfaces.

5 ACKNOWLEDGMENT

REFERENCES

Dees, S.L. (2001), *Spatial mechanism design using an svd-based distance metric*, Master's Thesis, Florida Institute of Technology.

Duffy, J. (1980), Analysis of mechanisms and robot manipulators, John Wiley & Sons.

Kihonge, J., Vance, J. and Larochelle, P. (2002), Spatial Mechanism Design in Virtual Reality with Networking, *ASME Journal of Mechanical Design (in press)*.

Larochelle, P. (2000), Circuit and branch rectification of the spatial 4c mechanism, *Proceedings of the ASME Design Engineering Technical Conferences*, Baltimore, USA.

Larochelle, P. (1998), Spades: software for synthesizing spatial 4c mechanisms, *Proceedings of the ASME Design Engineering Technical Conferences*, Atlanta, USA.

Larochelle, P. (1994), *Design of cooperating robots and spatial mechanisms*, PhD Dissertation, University of California, Irvine.

Marble, S., and Pennock, G. (1998), A study of the coupler curves of the rccc spatial four-bar mechanism, *Proceedings of the World Congress on the Theory of Machines and Mechanisms*, Oulu, Finland.

Murray, A.P., and Larochelle, P. (1998), A classification scheme for planar 4r, spherical 4r, and spatial rccc linkages to facilitate computer animation, *Proceedings of the ASME Design Engineering Technical Conferences*, Atlanta, USA.
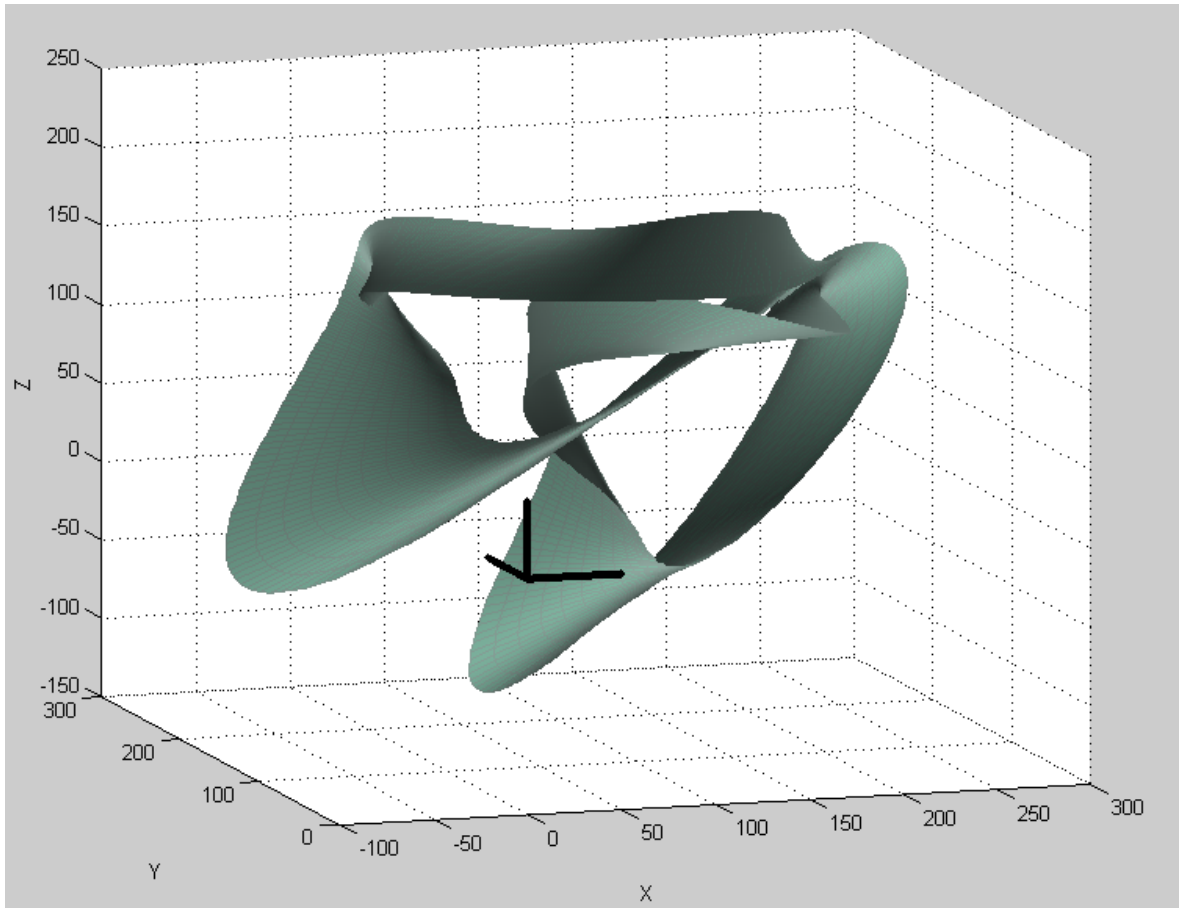
Figure 3.   SPATIAL 4C CRANK-ROCKER COUPLER SURFACES
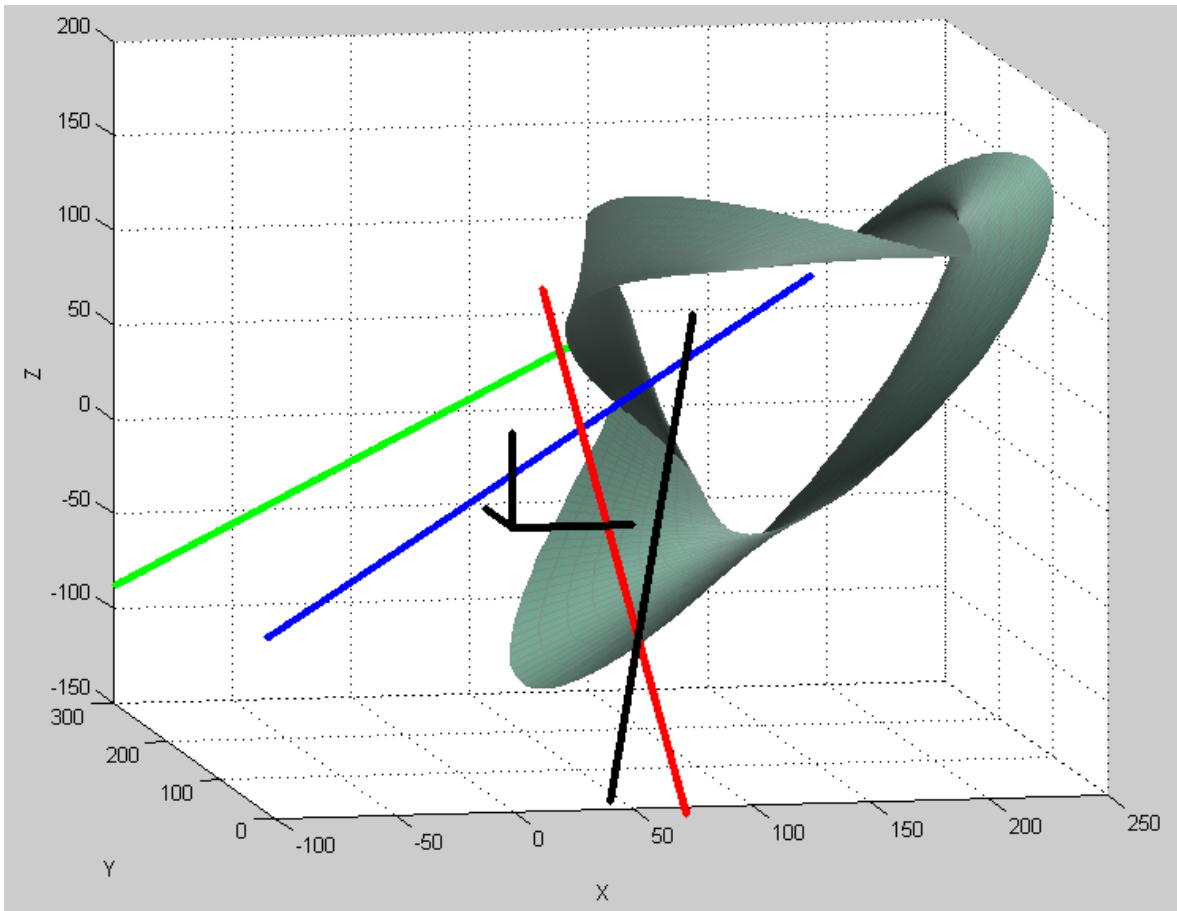
Figure 4.   SPATIAL 4C CRANK-ROCKER: ONE COUPLER SURFACE WITH JOINT AXES
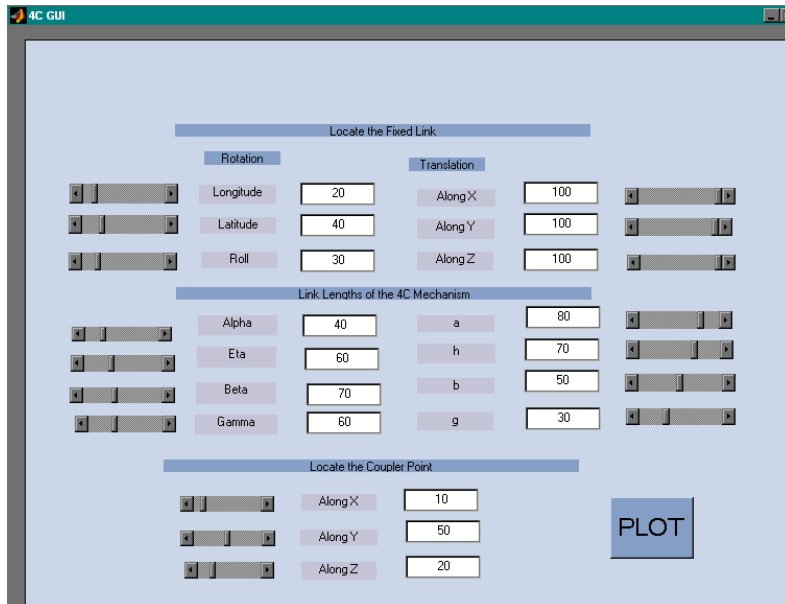
Figure 5.   CRANK-ROCKER MECHANISM DATA AND USER INTERFACE
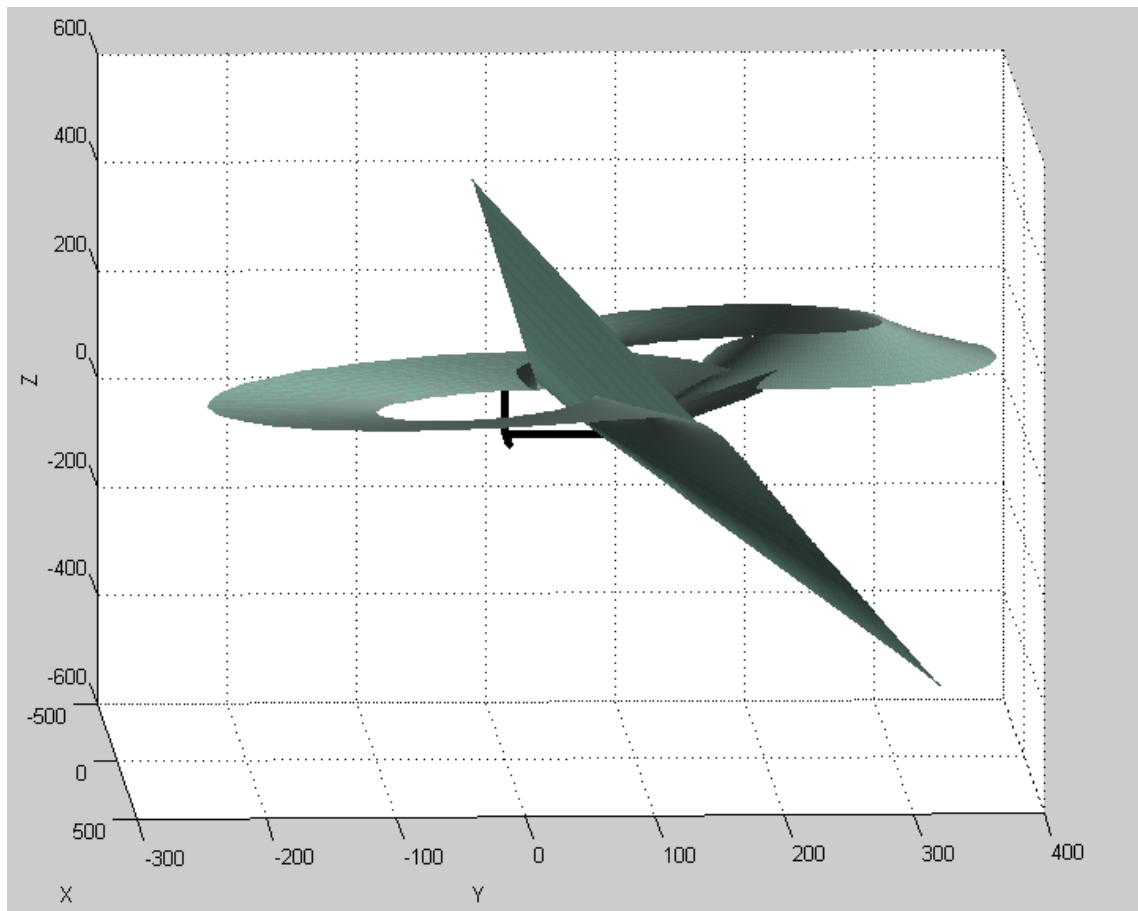
Figure 6.   SPATIAL 4C DOUBLE-ROCKER COUPLER SURFACE
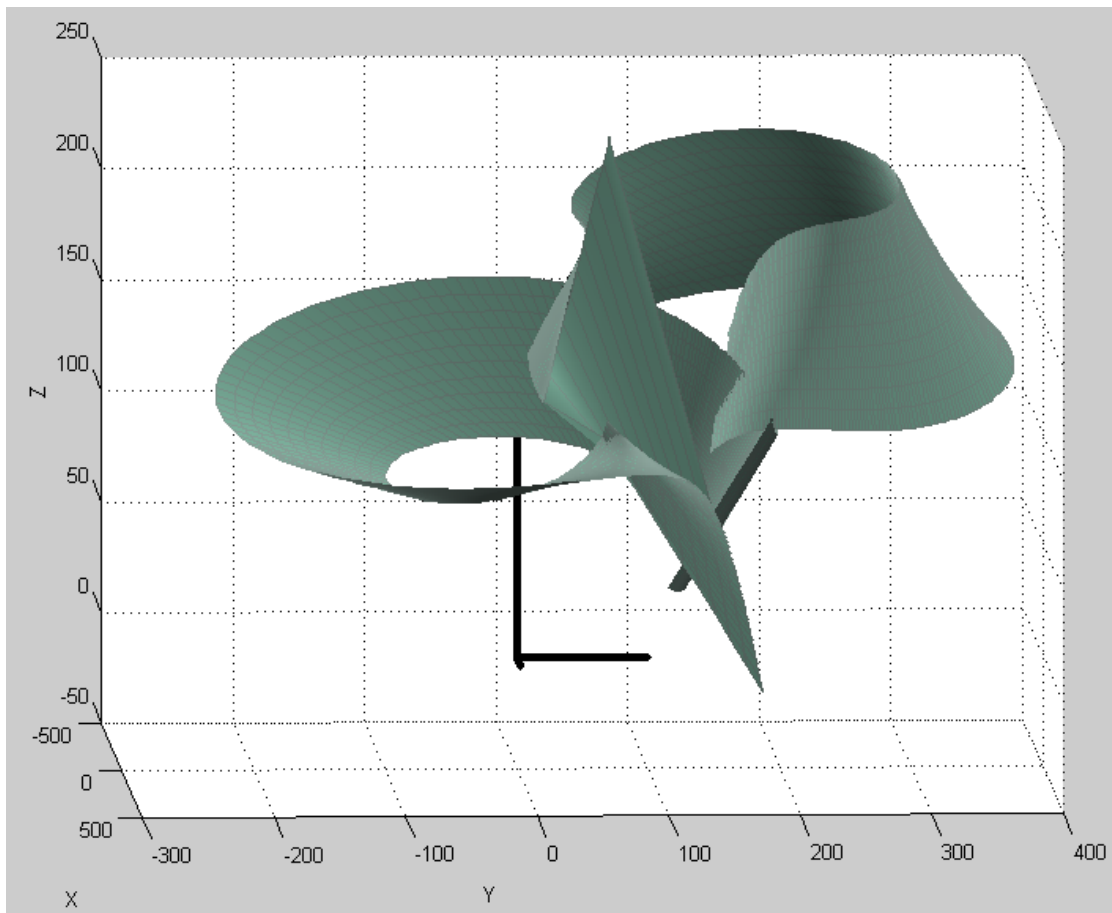
Figure 7.　SPATIAL 4C DOUBLE-ROCKER COUPLER SURFACE: MODIFIED θ RANGE
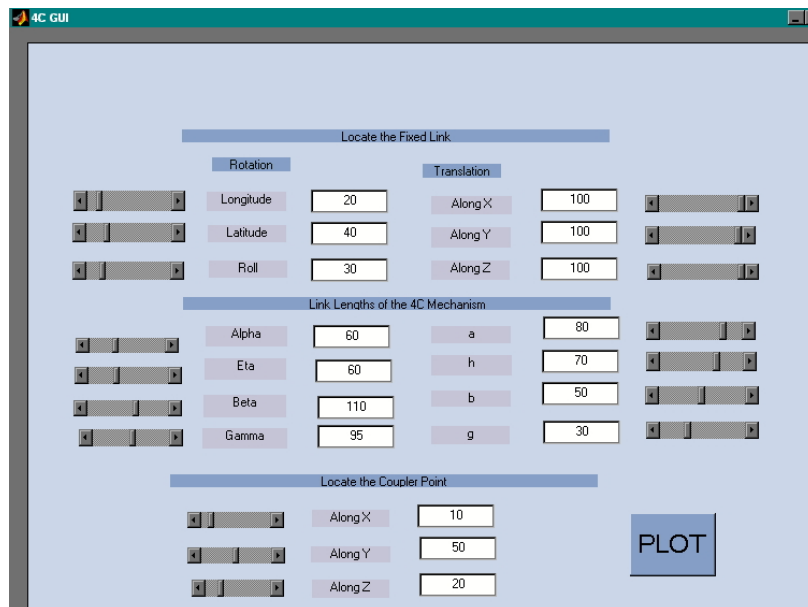
Figure 8.　DOUBLE-ROCKER MECHANISM DATA AND USER INTERFACE